

**Ab initio MO and quasi-classical direct ab initio MD studies
on the nitrogen inversion of trimethylamine**

Masato Tanaka, Misako Aida *

*Center for Quantum Life Sciences and Department of Chemistry, Graduate School of
Science, Hiroshima University, Kagamiyama, Higashi-Hiroshima, 739-8526 Japan*

Received 16 August 2005; in final form 28 September 2005

Abstract

A coupled motion of the skeletal inversion and methyl torsion in trimethylamine is investigated theoretically at various levels up to MP4(SDQ)/aug-cc-pVTZ. Among possible structures, the pyramidal C_{3v} is the only minimum energy structure, and the planar C_s is the transition state structure of the nitrogen inversion. Our best estimate of the barrier height (without zero-point energy) is 3290 cm^{-1} . The quasi-classical direct ab initio MD using HF/6-31G* starting from the pyramidal C_{3v} structure indicates that the coupled methyl torsional motion is the primary factor for the nitrogen inversion of trimethylamine.

* Corresponding author. FAX: +81-82-424-0725
e-mail address: maida@hiroshima-u.ac.jp (Misako Aida).

1. Introduction

The inversion of ammonia has been the subject of experimental and theoretical studies for many years. This is a prototype of the double-minimum potential and tunneling. The barrier height at D_{3h} is estimated to be $\approx 1900 \text{ cm}^{-1}$ (23 kJ/mol) [1, 2]. The potential energy surface for trimethylamine (TMA) is much more complex, being coupled by the torsional motion of three methyl groups. In spite of several theoretical works [3-6], the inversion process has never been clarified. Nor is there any experimental report on the transition state structure or the process of inversion except that the barrier height was estimated to be $\approx 2900 \text{ cm}^{-1}$ (35 kJ/mol) [7].

Methyl groups are ubiquitous in nature, and methyl torsions often play important roles in chemical and biochemical reactions. Here, we present ab initio MO calculations and a preliminary quasi-classical direct ab initio MD simulation to show that the torsion of the methyl groups is important in the nitrogen inversion process of TMA.

2. Methods

Ab initio MO calculations were carried out using analytic gradients at the Hartree-Fock (HF) level with 6-31G* basis set [8-10], as well as the Møller-Plesset [11] electron correlation energy correction, truncated at the second-order (MP2) with 6-31G*, aug-cc-pVDZ and aug-cc-pVTZ basis sets [12] and at the fourth-order with single, double and quadruple substitutions, MP4(SDQ) [13], with aug-cc-pVTZ basis set. Local minima and transition state structures were identified by a full analysis of the vibrational modes using analytical second derivatives for HF/6-31G*, MP2/6-31G*, MP2/aug-cc-pVDZ and MP2/aug-cc-pVTZ. Intrinsic reaction coordinate (IRC) [14,

15] calculations were also done. The program packages used were HONDO-2003 [16], Gaussian03 [17] and GAMESS [18].

A quasi-classical direct ab initio MD simulation [19] was carried out at the level of HF/6-31G* with a time step of 0.2fs and with the constant total energy, in which some quantum energies were assigned to the out-of-plane and the methyl torsion modes. The program package used for the simulations was HONDO-2003.

3. Results and discussion

3-1. Structures of trimethylamine

Figure 1 and Table 1 show the molecular structures and the relative energies, respectively, of all the stationary points that we have found. As for the pyramidal structures, we find that structure A (*pyr-C_{3v}*) is the most stable and structure B (*pyr-C_s*) is the transition state of the torsion of one methyl group. The barrier height of one-methyl torsion is $\approx 1400 \text{ cm}^{-1}$ (17 kJ/mol) in the pyramidal structure, which is consistent with the experimentally predicted barrier heights of methyl torsion [20]. No other stationary points are found in the pyramidal geometry.

The transition state of the skeletal inversion of TMA should have a planar structure. Structure C (*pla-C_s*) corresponds to this transition state, as indicated by the numbers of imaginary frequencies (Table 1). Our best estimate of the barrier height (without account of zero-point energy, ZPE) for the inversion is 3290 cm^{-1} (39.4 kJ/mol) at MP4(SDQ)/aug-cc-pVTZ. As shown in Table 1, the barrier height is overestimated with the MP2 method. The estimate with HF/6-31G*, 34.9 kJ/mol, is accidentally coincident with the experimental value, $\approx 2900 \text{ cm}^{-1}$ (35 kJ/mol) [7]. The relative energy including ZPE is $\approx 5 \text{ kJ/mol}$ lower than the barrier height by any method listed

here. The theoretical barrier height is the one for the full potential energy surface, while the experimental ‘barrier height’ is the one for the one-dimensional potential along the postulated inversion coordinate [7]; the latter may implicitly include the ZPE of the other modes. For this reason, the theoretical barrier height at MP4(SDQ)/aug-cc-pVTZ is inconsistent with the experimentally estimated value.

3-2. IRC of inversion

The IRC calculations were performed to confirm that *pla-Cs* is the transition state structure of the skeletal inversion between *pyr-C_{3v}*. The degree of inversion d is defined as shown in Fig. 2. The sign is added to distinguish between the initial and final stages of inversion, where $d = \pm 1$ corresponds to *pyr-C_{3v}*. We project the geometrical change along the IRC on the d value. The energy changes along the IRC paths based on MP2/aug-cc-pVDZ and HF/6-31G* are plotted in Fig. 3 in terms of d with a schematic view of the methyl motions. Both computational levels show qualitatively the same inversion process.

It is worthy of note that the methyl torsions along the IRC correspond to one of the degenerate ν_{22} $\tau(\text{CH}_3)$ mode (e) of TMA [21], in which two of the methyl torsions are identical while the other is different. Another methyl torsional mode of TMA is the ν_{11} $\tau(\text{CH}_3)$ mode (a₂), in which three methyl torsions are identical. If the motion of the methyl groups were along the ν_{11} mode in the inversion process, the planar structure should be structure D (*pla-C_{3h}*). As shown in Table 1, however, *pla-C_{3h}* is *not* the transition state of the nitrogen inversion. Therefore, the route with methyl torsions along the ν_{11} mode through *pla-C_{3h}* should be different from the IRC.

3-3. Comparison of the IRC path with experimental double-minimum potentials

The absorption and the fluorescence spectra of TMA were reproduced [7] by use of the one-dimensional double-minimum potential of inversion for the ground state and the harmonic single-well potential for the excited state. The following two simplifying assumptions were made in this procedure: (a) The methyl groups were treated as point masses, and (b) the C–N bond lengths were assumed to be equal and constant. Thus, the model potential of the nitrogen inversion for the ground state was derived using two local parabolic wells corresponding to the out-of-plane bending mode, the ν_7 ($\delta_s\text{NC}_3$) mode (a_1), of *pyr*- C_{3v} smoothly joined by either a quadratic or a quartic cap which functioned as the inversion barrier height.

This experimental model potential is compared in Fig. 4 with our IRC path at the HF/6-31G* level. The curvature of the quadratic cap is almost identical to that of the IRC path around the inversion transition state, while the bottom of the potential significantly deviates from the IRC path. In Fig. 4, a path in which the atoms move only along the out-of-plane bending mode and the C_{3v} symmetry is conserved is plotted (C_{3v} path) from *pyr*- C_{3v} toward the planar C_{3v} structure (*pla*- C_{3v}). Although it is not the stationary point, the energy of *pla*- C_{3v} is ≈ 2 kJ/mol lower than that of *pla*- C_s using any theoretical level (data not shown here). It should be noted that the potential energy is lower on the C_{3v} path than that on the IRC path. After passing the planar structure along the C_{3v} path, the energy is raised because of the repulsion between the methyl groups, and this C_{3v} path is not led to another stable conformer. The inversion process must couple with the methyl group torsions from the early stage of the inversion, even though the coupling needs extra energy. In the experimental model potential, the bottom of the potential is simply the out-of-plane bending mode without methyl group

torsions; the quadratic cap practically serves to include the methyl torsions in the inversion path and makes the path close to the IRC path.

3-4. *Quasi-classical direct ab initio MD trajectories*

The IRC path is a hypothetical path in which the atoms move with zero velocities. A reaction path corresponding to the atomic motion with a finite velocity is in principle different from the IRC path. Hence, quasi-classical direct ab initio MD simulations with constant total energy were performed, in which we included the initial velocities consistent with the oscillator amplitudes with vibrational potential energy equal to PE [19],

$$\text{PE} = hc \sum_i \tilde{\nu}_i \left(n_i + \frac{1}{2} \right), \quad (1)$$

where $\tilde{\nu}_i$ is the harmonic wavenumber of the i -th mode, n_i is the quantum number of the i -th mode, h is Planck's constant and c is the light velocity. We tested several combinations of the modes (to which the vibrational potential energies were added) and the quantum numbers (in correspondence with the amount of the added energy).

Preliminary results are shown here. We started simulations from the minimum energy structure (*pyr-C_{3v}*). No inversion was observed (data not shown here) when thermal energy exceeding the barrier height was added to the system in which the atoms move at random, or when excess energy is added to the out-of-plane mode only. We have confirmed, however, that the inversion does occur when excess energy is added to both the out-of-plane (ν_7) mode and one of the degenerate ν_{22} mode of the methyl torsions. Figure 5 shows the potential energy change of the trajectory projected onto the degree of inversion d during 10000 steps (2000 fs) of the MD run. In this case, the vibrational potential energy is 4200 cm^{-1} (50 kJ/mol), which is the sum of $n_{\text{methyl}} = 6$

($\tilde{\nu}_{\text{methyl}} = 284.6 \text{ cm}^{-1}$) and $n_{\text{out-of-plane}} = 6$ ($\tilde{\nu}_{\text{out-of-plane}} = 383.6 \text{ cm}^{-1}$). In Fig. 5, the experimental potential curve with the quadratic cap [7] is plotted with dotted line. It is seen that the atoms oscillate in two basins and the barrier is crossed only once. For chemical reactions, the use of the concept of a single, nearly separable reactive degree of freedom in the system's phase space was strongly supported [22]. Note that the degree of inversion d is not the reactive degree in this case. It is probable that an adequate combination with the methyl torsions serves as the primary reactive degree. The conditions of feasible barrier crossing are the target of our current simulations.

4. Summary

The HF/6-31G* calculation has reproduced the potential energy surface of the nitrogen inversion of TMA. The quasi-classical direct ab initio MD simulation at the level of HF/6-31G* has shown that a specific torsional mode of the methyl groups (one of the degenerate ν_{22} $\tau(\text{CH}_3)$ mode) is strongly coupled with the mode of nitrogen inversion.

Acknowledgments

The calculations were carried out in part at the Research Center for Computational Science, Okazaki National Research Institutes. This study was partly supported by grants from the Ministry of Education, Culture, Sports, Science and Technology of Japan.

References

- [1] A.M. Halpern, E.D. Glendening, *Chem. Phys. Lett.* 333 (2001) 391.
- [2] V. Špirko, W.P. Kraemer, *J. Mol. Spectrosc.* 133 (1989) 331.
- [3] C. M.B. Marsh, H.F. Schaefer III, *J. Phys. Chem.* 99 (1995) 195.
- [4] R.A. Eades, D.A. Weil, D.A. Dixon, C.H. Douglass, Jr., *J. Phys. Chem.* 85 (1981) 976.
- [5] C. Kölmel, C. Ochsenfeld, R. Ahlrichs, *Theor. Chim. Acta* 82 (1991) 271.
- [6] Y. Mo, Y. Zhang, J. Gao, *J. Am. Chem. Soc.* 121 (1999) 5737.
- [7] A.M. Halpern, M.J. Ondrechen, L.D. Ziegler, *J. Am. Chem. Soc.* 108 (1986) 3907.
- [8] W. J. Hehre, R. Ditchfield, J.A. Pople, *J. Chem. Phys.* 56 (1972) 2257.
- [9] J.D. Dill, J.A. Pople, *J. Chem. Phys.* 62 (1975) 2921.
- [10] P.C. Hariharan, J.A. Pople, *Theor. Chim. Acta* 28 (1973) 213.
- [11] C. Møller, M.C. Plesset, *Phys. Rev.* 46 (1934) 618.
- [12] T.H. Dunning, Jr., *J. Chem. Phys.* 90 (1989) 1007.
- [13] G.W. Trucks, E.A. Salter, C. Sosa, R.J. Bartlett, *Chem. Phys. Lett.* 147 (1988) 359.
- [14] K. Fukui, *J. Phys. Chem.* 74 (1970) 4161.
- [15] C. Gonzales, H.B. Schlegel, *J.Chem.Phys.* 90 (1989) 2154.
- [16] M. Dupuis, HONDO-2003, Based on HONDO-95 Available From the Quantum Chemistry Program Exchange, Indiana University, Bloomington, IN, USA (2003).
- [17] M.J. Frisch et al., *Gaussian 03, Revision C.02*, Gaussian, Inc., Wallingford CT, 2004.
- [18] M.W. Schmidt, K.K. Baldridge, J.A. Boatz, S.T. Elbert, M.S. Gordon, J.H. Jensen, S. Koseki, N. Matsunaga, K.A. Nguyen, S. Su, T.L. Windus, M. Dupuis, J.A.

Montgomery, Jr, J. Comput. Chem. 14 (1993) 1347.

[19] M. Aida, M. Dupuis, Chem. Phys. Lett. 401 (2005) 170.

[20] J.R. Durig, S.M. Craven, J. Bragin, J. Chem. Phys. 53 (1970) 38.

[21] W.F. Murphy, F. Zerbetto, J.L. Duncan, D.C. McKean, J. Phys. Chem. 97 (1993) 581.

[22] T. Komatsuzaki, R.S. Berry, J. Phys. Chem. A 106 (2002) 10945.

[23] H. Fujiwara, T. Egawa, S. Konaka, J. Mol. Struct. 344 (1995) 217.

Table 1 Calculated relative energies^a of various structures^b of trimethylamine

	<u>pyramidal</u>		<u>planar</u>	
	<i>pyr-C_{3v}</i>	<i>pyr-C_s</i>	<i>pla-C_s</i>	<i>pla-C_{3h}</i>
HF/6-31G*	0.0 (0.0) {0}	18.0 (16.4) {1}	34.9 (29.7) {1}	37.3 (30.5) {3}
MP2/6-31G*	0.0 (0.0) {0}	19.9 (18.5) {1}	42.3 (37.3) {1}	46.2 (39.1) {4}
MP2/aug-cc-pVDZ	0.0 (0.0) {0}	19.2 (18.1) {1}	45.2 (40.3) {1}	48.2 (41.5) {4}
MP2/aug-cc-pVTZ	0.0 (0.0) {0}	18.0 (17.6) {1}	41.5 (37.0) {1}	44.3 (38.0) {4}
MP4(SDQ) /aug-cc-pVTZ ^c	0.0	16.9	39.4	41.7

^a Energies of the stationary points are shown in kJ/mol relative to the pyramidal C_{3v} structure. Relative energies with ZPE corrected are shown in parentheses. Numbers of imaginary frequencies are shown in braces.

^b Structures are shown in Fig. 1.

^c Relative energies at MP3/aug-cc-pVTZ with the optimized geometries at MP4(SDQ) /aug-cc-pVTZ are 0.0, 16.7, 39.2 and 41.4 kJ/mol, respectively.

Figure captions

Fig. 1. Structures of TMA. (A) pyramidal C_{3v} , (B) pyramidal C_s , (C) planar C_s , and (D) planar C_{3h} structures.

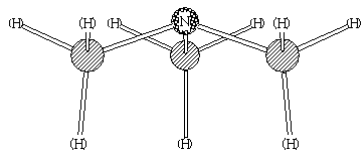
Fig. 2. Definition of the degree of inversion, d . Unit vectors e_i ($i=1,2,3$) are directed to each N–C bond. The height r is equal to r_{pyr} for the pyramidal C_{3v} structure and is 0 at the planar structure, where $r_{\text{pyr}} = 0.289, 0.325$ and 0.314 \AA at HF/6-31G*, MP2/aug-cc-pVDZ and MP4(SDQ)/aug-cc-pVTZ, respectively. Experimentally, a gas electron diffraction study of TMA [23] reported that $r_{\text{pyr}} = 0.314 \text{ \AA}$.

Fig. 3. Potential energy curves (in kJ/mol) of TMA along the IRC path at HF/6-31G* (solid line) and at MP2/aug-cc-pVDZ (broken line). The structures at the points of $d = -1.0, -0.5, 0.0, 0.5$ and 1.0 are shown.

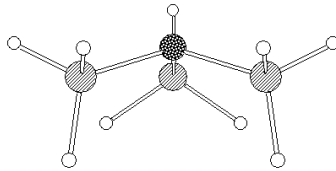
Fig. 4. Potential energy curves (in cm^{-1}) for the inversion of TMA. Thick solid line with filled circles is the present results of IRC at HF/6-31G*. Thin solid line with open circle is the C_{3v} path at HF/6-31G*. Thin solid line (parabolic) and thin dashed line (quartic) are experimental potentials [7]; the horizontal coordinate used in [7] is converted to d . The IRC path cannot be plotted for $|d| > 1$, since the IRC is defined between the transition state and the energy minimum structures. Note that the d value itself is not the reaction coordinate of the inversion.

Fig. 5. Potential energy change along the quasi-classical direct ab initio MD trajectory and the experimental potential curve (dotted line) are plotted in kJ/mol against d .

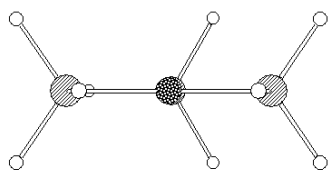
(A)



(B)



(C)



(D)

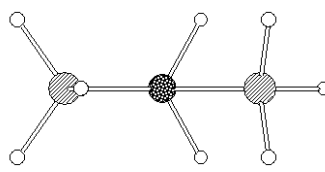
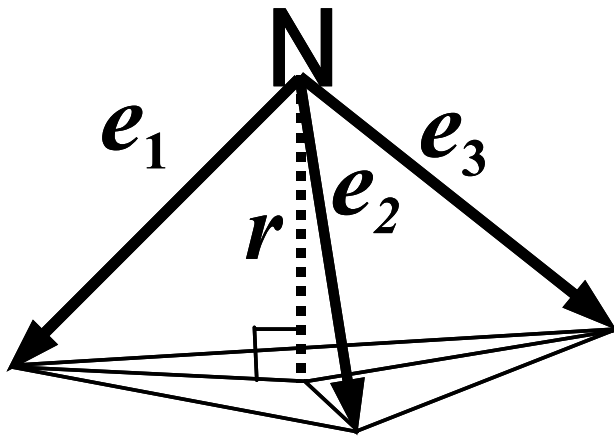


Fig. 1 (Tanaka & Aida)



$$|d| = \frac{r}{r_{\text{pyr}}}$$

Fig. 2 (Tanaka & Aida)

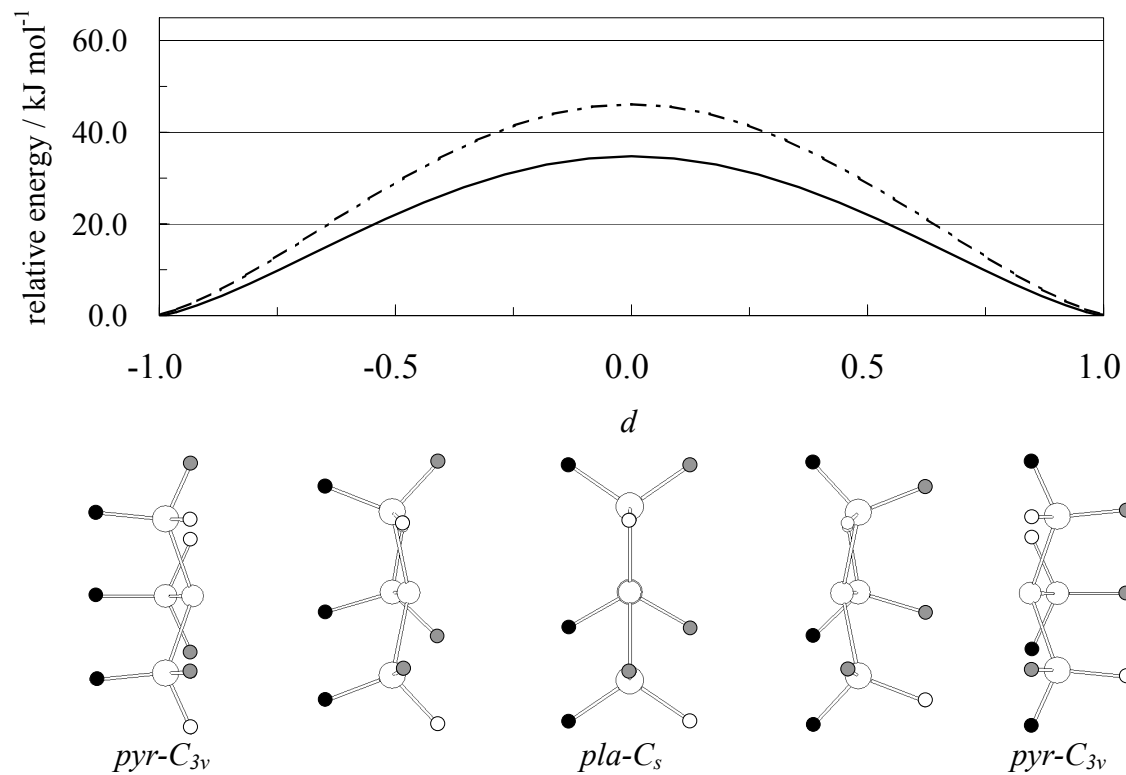


Fig. 3 (Tanaka & Aida)

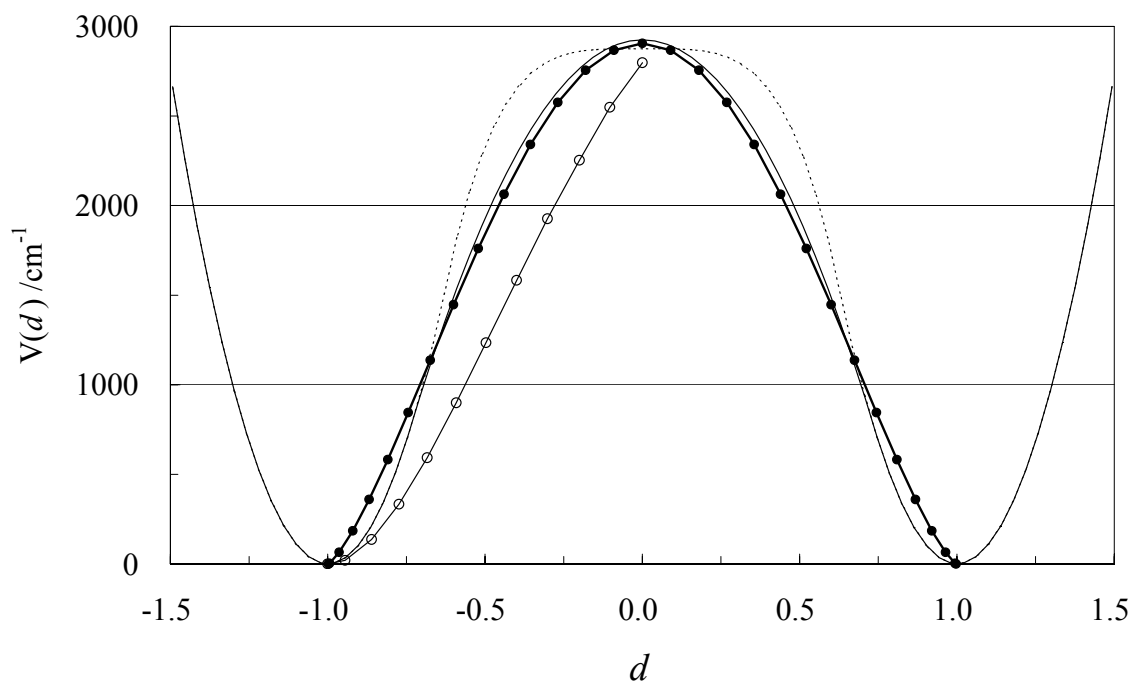


Fig. 4 (Tanaka & Aida)

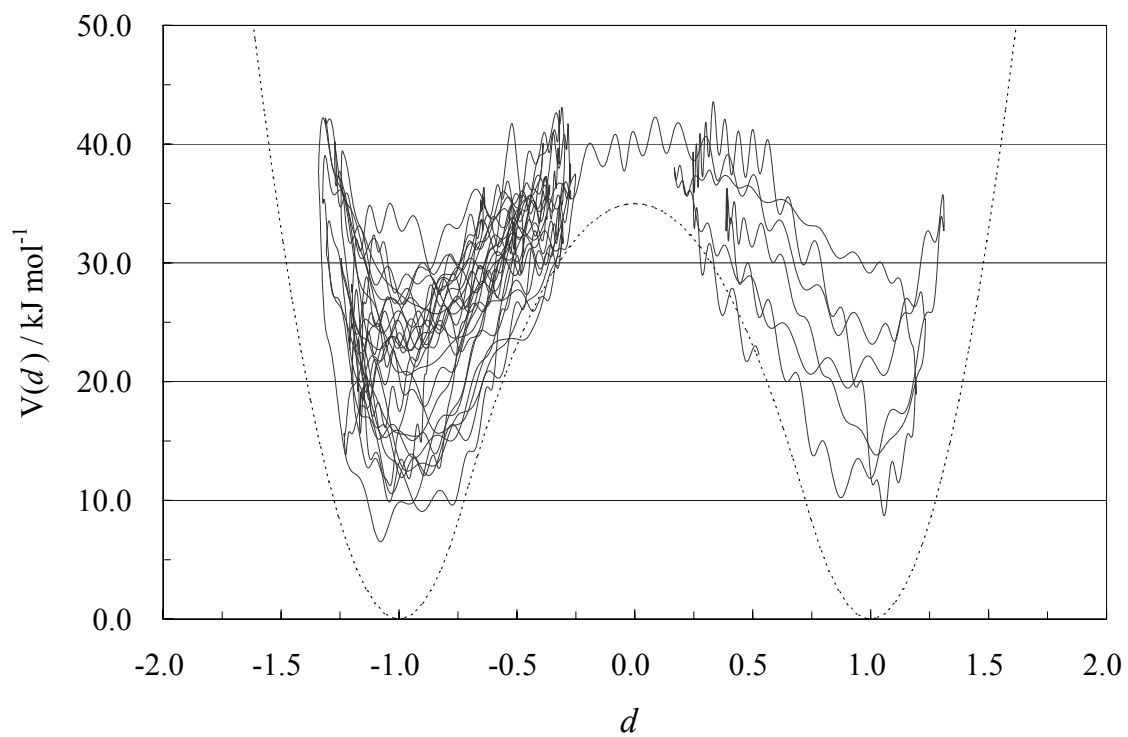


Fig. 5 (Tanaka & Aida)